

# Minimal models of the Solar cycle

Friedrich H Busse<sup>1,3</sup> and Radostin D Simatev<sup>2,3</sup>

<sup>1</sup> Institute of Physics, University of Bayreuth, Bayreuth D-95440, Germany

<sup>2</sup> School of Mathematics & Statistics, University of Glasgow, Glasgow G12 8QW, UK

<sup>3</sup> NORDITA, AlbaNova University Center, Stockholm SE-10691, Sweden

E-mail: Busse@uni-bayreuth.de, Radostin.Simatev@glasgow.ac.uk

**Abstract.** We discuss the extent to which minimal self-consistent models of convection-driven dynamos may reproduce the Solar cycle.

PACS numbers: ?? ?? ?? (specify here)

1. Figures dated - 03 Jan 2011

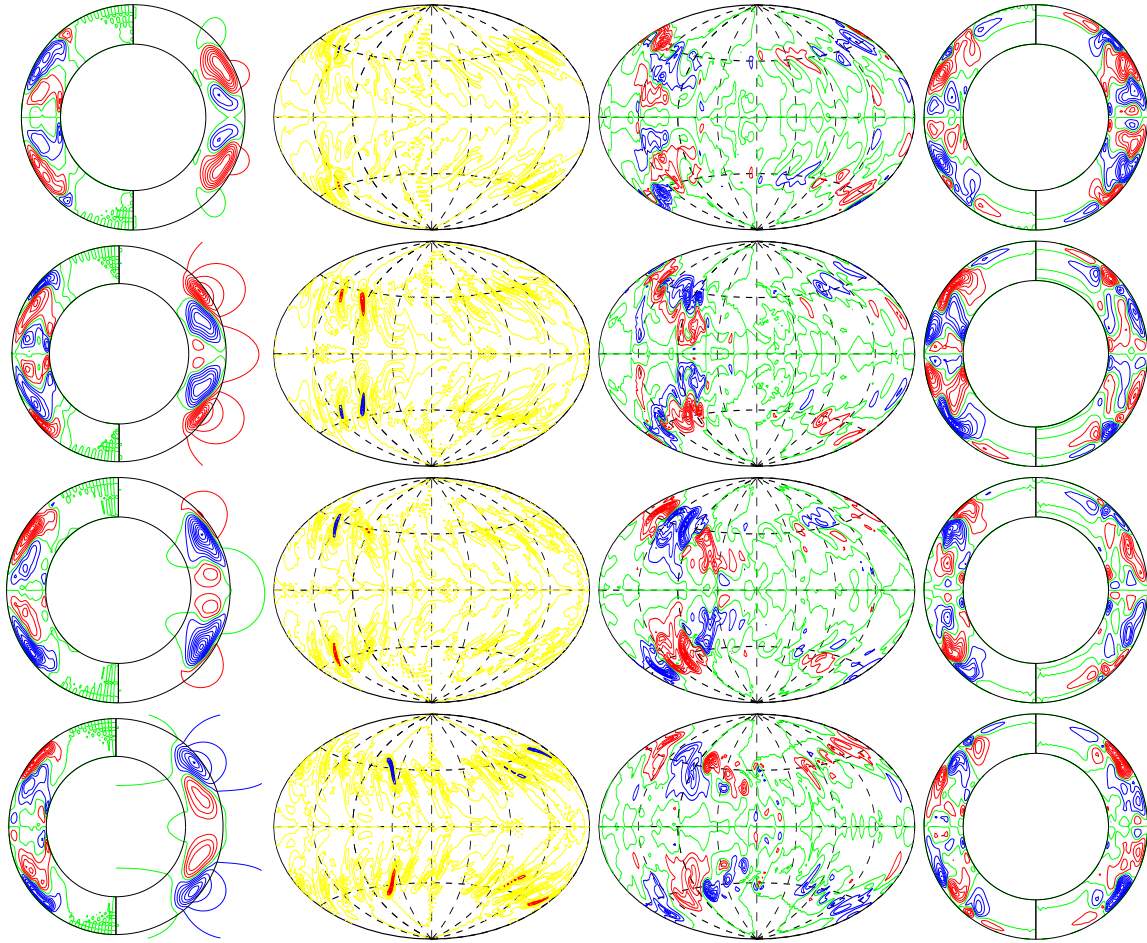


Figure 18: (color online) A dynamo oscillation in the case  $\tau = 2000$ ,  $R = 150000$ ,  $P = 1$ ,  $P_m = 4.5$ ,  $\beta = 0$ , stress-free at  $r_o$  and no-slip at  $R - i$ . The first column shows meridional lines of constant  $\overline{B}_\varphi$  on the left and poloidal field lines,  $r \sin \theta \partial \overline{h} / \partial \theta$  on the right. The second column shows lines of constant  $\partial g / \partial \theta$  at  $r = 0.9$  corresponding to  $-0.9, -0.8, -0.7, 0.7, 0.8, 0.9$  of the maximum absolute value of  $\partial g / \partial \theta$ , and the third column shows lines of constant  $B_r$  at  $r = r_o$ . The last column shows  $\text{Re}(\partial g^{m=2} / \partial \theta)$  on the left and  $\text{Im}(\partial g^{m=2} / \partial \theta)$  on the right. The five rows are separated equidistantly in time by  $\Delta t = 0.028$ .

e065p1t2r150000m1p4.5mvbcFD

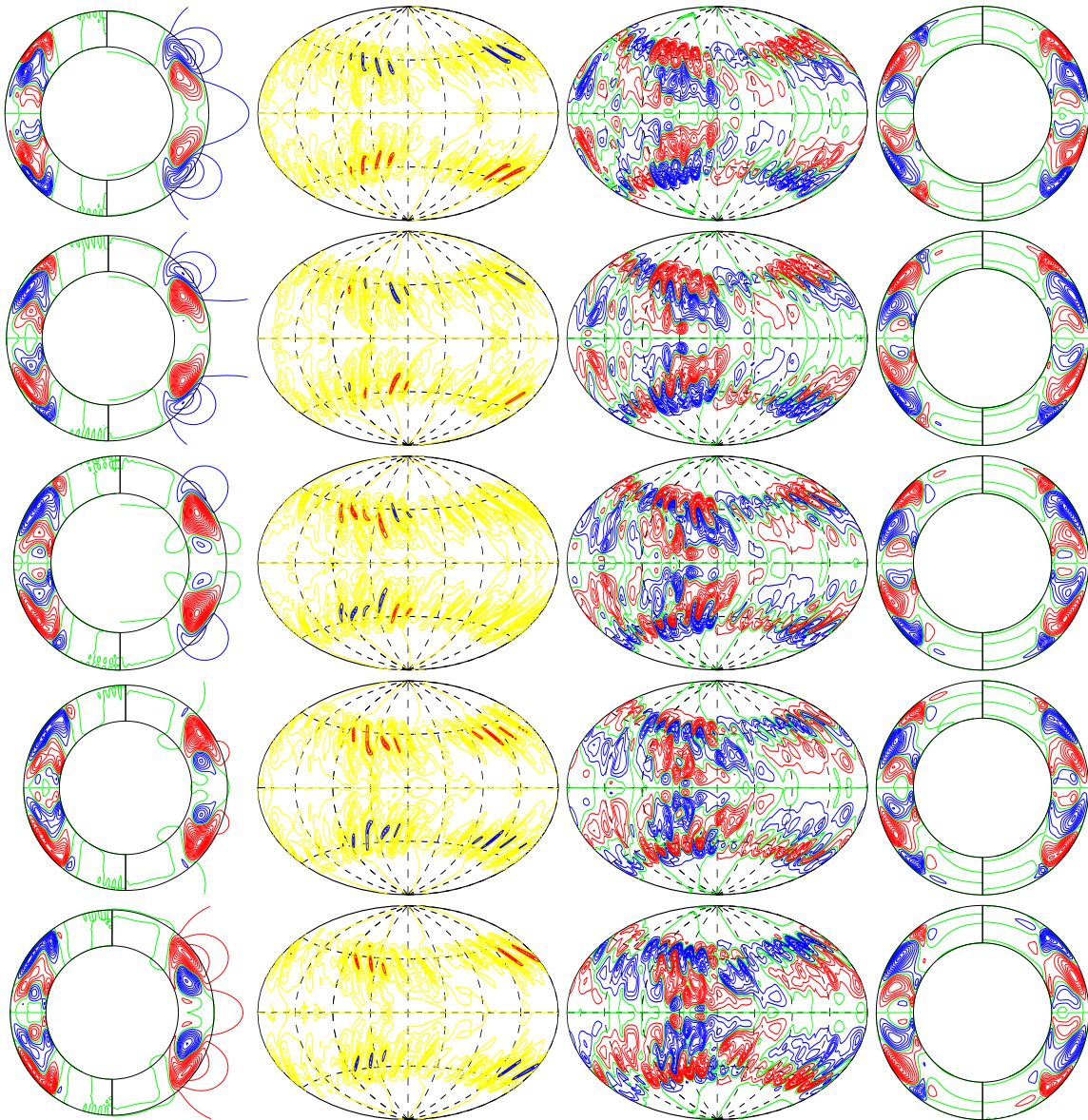


Figure 19: (color online) A dynamo oscillation in the case  $\tau = 2000$ ,  $R = 110000$ ,  $P = 1$ ,  $P_m = 4.5$ ,  $\beta = 0$ , stress-free at  $r_o$  and no-slip at  $R - i$ . The first column shows meridional lines of constant  $\overline{B}_\varphi$  on the left and poloidal field lines,  $r \sin \theta \overline{dh}/\partial\theta$  on the right. The second column shows lines of constant  $\partial g/\partial\theta$  at  $r = 0.9$  corresponding to  $-0.9, -0.8, -0.7, 0.7, 0.8, 0.9$  of the maximum absolute value of  $\partial g/\partial\theta$ , and the third column shows lines of constant  $B_r$  at  $r = r_o$ . The last column shows  $\text{Re}(\partial g^{m=2}/\partial\theta)$  on the left and  $\text{Im}(\partial g^{m=2}/\partial\theta)$  on the right. The five rows are separated equidistantly in time by  $\Delta t = 0.0168$ .

e065p1t2r110000m1p4.5mvbcFD

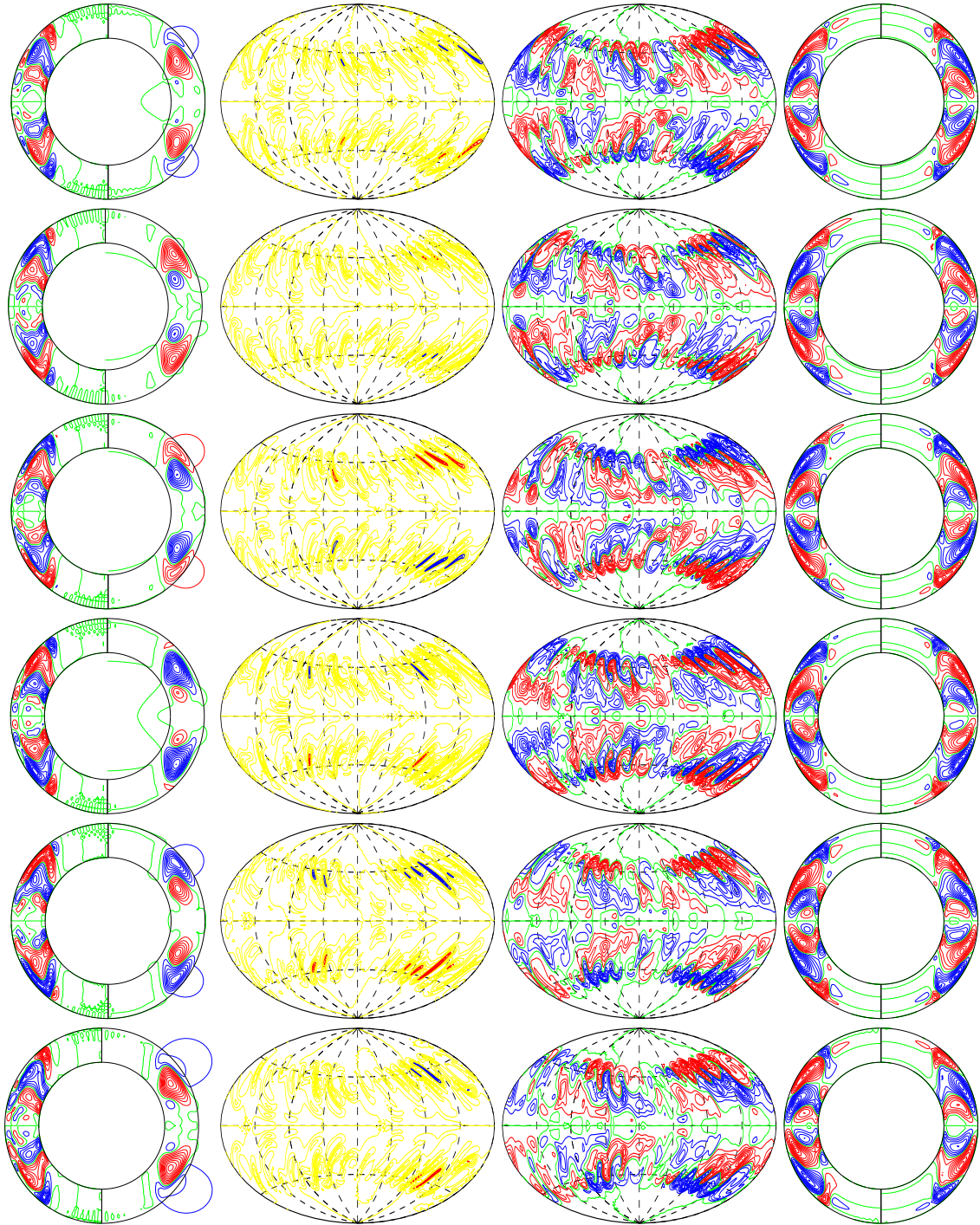


Figure 20: (color online) A dynamo oscillation in the case  $\tau = 2000$ ,  $R = 100000$ ,  $P = 1$ ,  $P_m = 6$ ,  $\beta = 0$ , stress-free at  $r_o$  and no-slip at  $R - i$ . The first column shows meridional lines of constant  $\overline{B_\varphi}$  on the left and poloidal field lines,  $r \sin \theta \overline{\partial h} / \partial \theta$  on the right. The second column shows lines of constant  $\partial g / \partial \theta$  at  $r = 0.9$  corresponding to  $-0.9, -0.8, -0.7, 0.7, 0.8, 0.9$  of the maximum absolute value of  $\partial g / \partial \theta$ , and the third column shows lines of constant  $B_r$  at  $r = r_o$ . The last column shows  $\text{Re}(\partial g^{m=2} / \partial \theta)$  on the left and  $\text{Im}(\partial g^{m=2} / \partial \theta)$  on the right. The five rows are separated equidistantly in time by  $\Delta t = 0.028$ .

e065p1t2r100000m1p6mvbcB

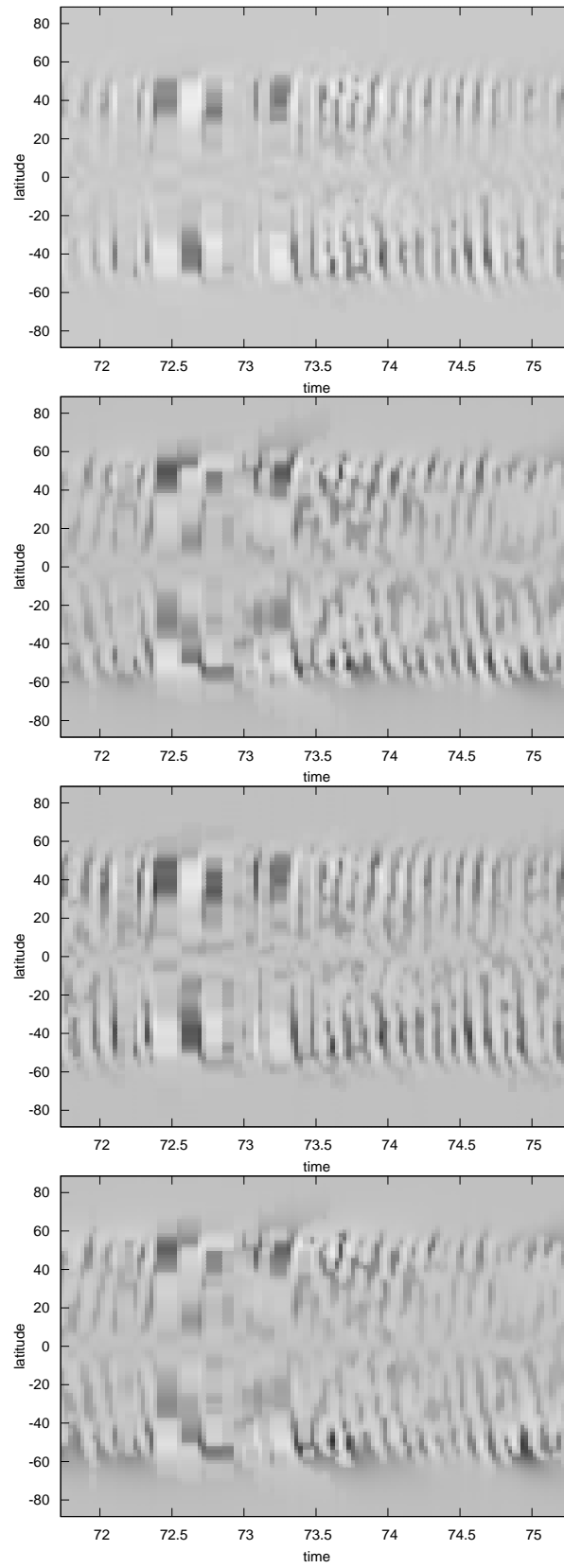


Figure 21: “Butterfly” diagrams:  $B_\varphi^{m=0} + |B_\varphi^{m=1}| \text{sgn}(B_\varphi^{m=0})$ ,  $B_r^{m=0} + |B_r^{m=1}| \text{sgn}(B_r^{m=0})$ ,  $B_\varphi^{m=0} + |B_\varphi^{m=2}| \text{sgn}(B_\varphi^{m=0})$ ,  $B_r^{m=0} + |B_r^{m=2}| \text{sgn}(B_r^{m=0})$ , (from top to bottom) are plotted as functions of latitude and time in the case  $P = 1$ ,  $\tau = 2000$ ,  $R = 150000$ ,  $P_m = 4.5$ .

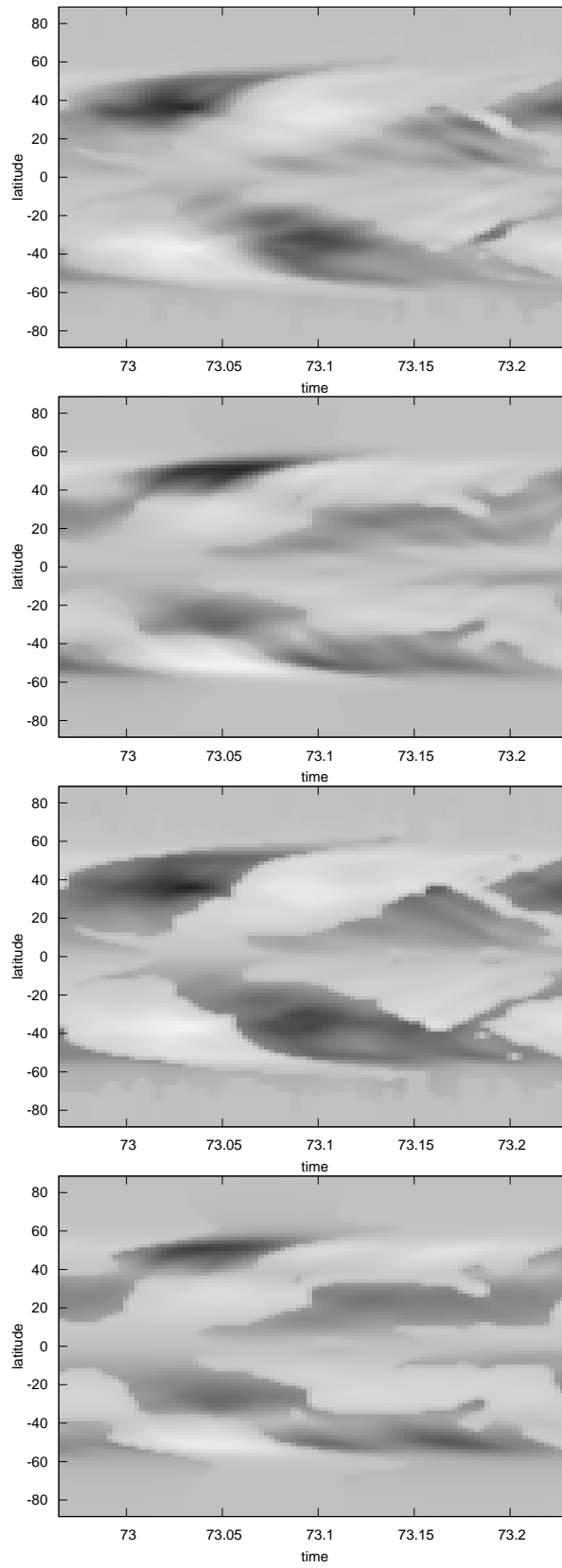


Figure 22: “Butterfly” diagrams:  $B_\varphi^{m=0} + |B_\varphi^{m=1}| \text{sgn}(B_\varphi^{m=0})$ ,  $B_r^{m=0} + |B_r^{m=1}| \text{sgn}(B_r^{m=0})$ ,  $B_\varphi^{m=0} + |B_\varphi^{m=2}| \text{sgn}(B_\varphi^{m=0})$ ,  $B_r^{m=0} + |B_r^{m=2}| \text{sgn}(B_r^{m=0})$ , (from top to bottom) are plotted as functions of latitude and time in the case  $P = 1$ ,  $\tau = 2000$ ,  $R = 110000$ ,  $P_m = 4.5$ .

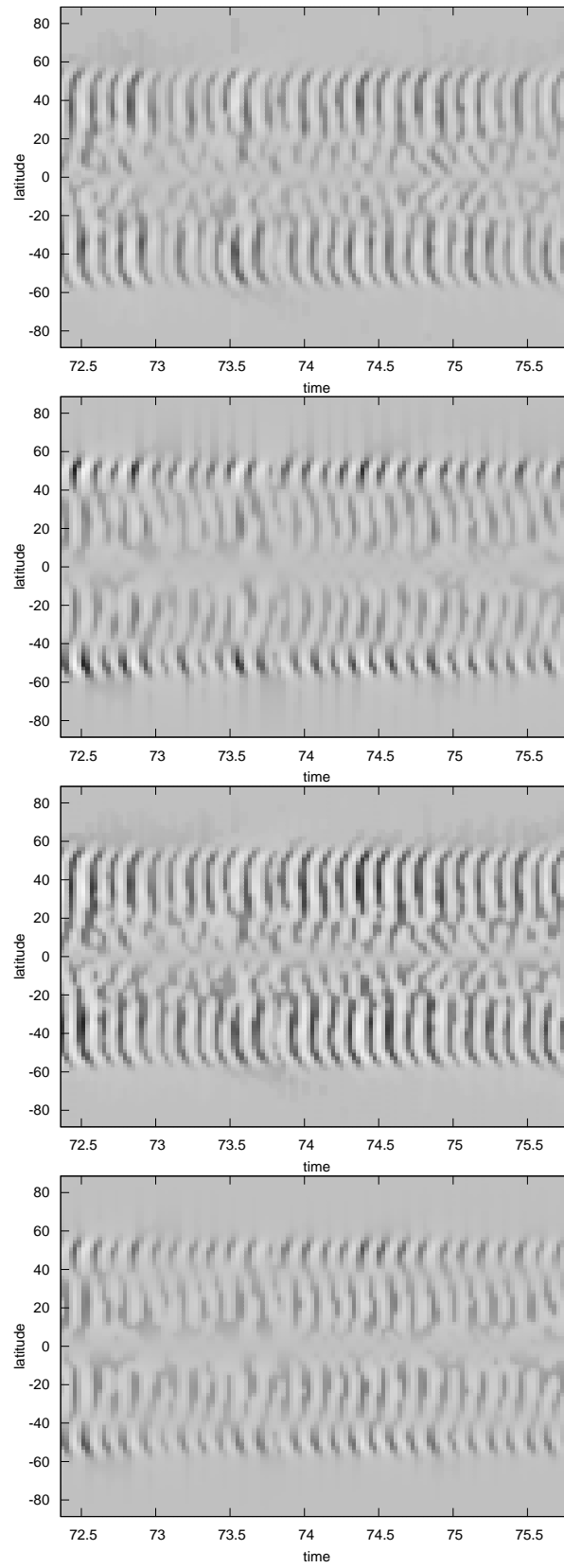
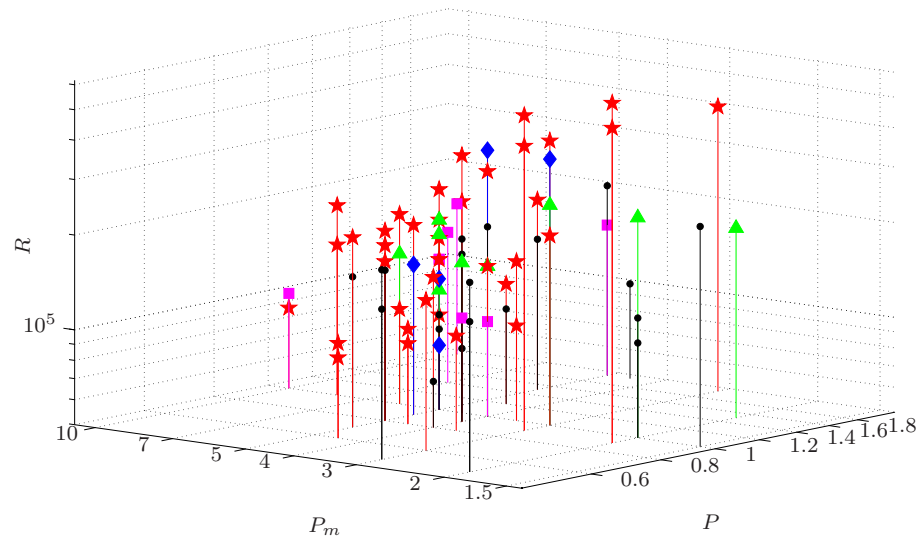


Figure 23: “Butterfly” diagrams:  $B_\varphi^{m=0} + |B_\varphi^{m=1}| \text{sgn}(B_\varphi^{m=0})$ ,  $B_r^{m=0} + |B_r^{m=1}| \text{sgn}(B_r^{m=0})$ ,  $B_\varphi^{m=0} + |B_\varphi^{m=2}| \text{sgn}(B_\varphi^{m=0})$ ,  $B_r^{m=0} + |B_r^{m=2}| \text{sgn}(B_r^{m=0})$ , (from top to bottom) are plotted as functions of latitude and time in the case  $P = 1$ ,  $\tau = 2000$ ,  $R = 100000$ ,  $P_m = 6$ .



clip clip

Figure 24: Convection-driven dynamos as a function of  $R$ ,  $P$  and  $P_m$  for  $\tau = 2000$  and  $\eta = 0.6, 0.65$ . Decaying dynamos are indicated by black dots, MD dynamos are indicated by blue diamonds, FD dynamos are indicated by red stars, quadrupolar dynamos are indicated by green triangles, and coexisting MD and FD dynamos are indicated by pink squares.

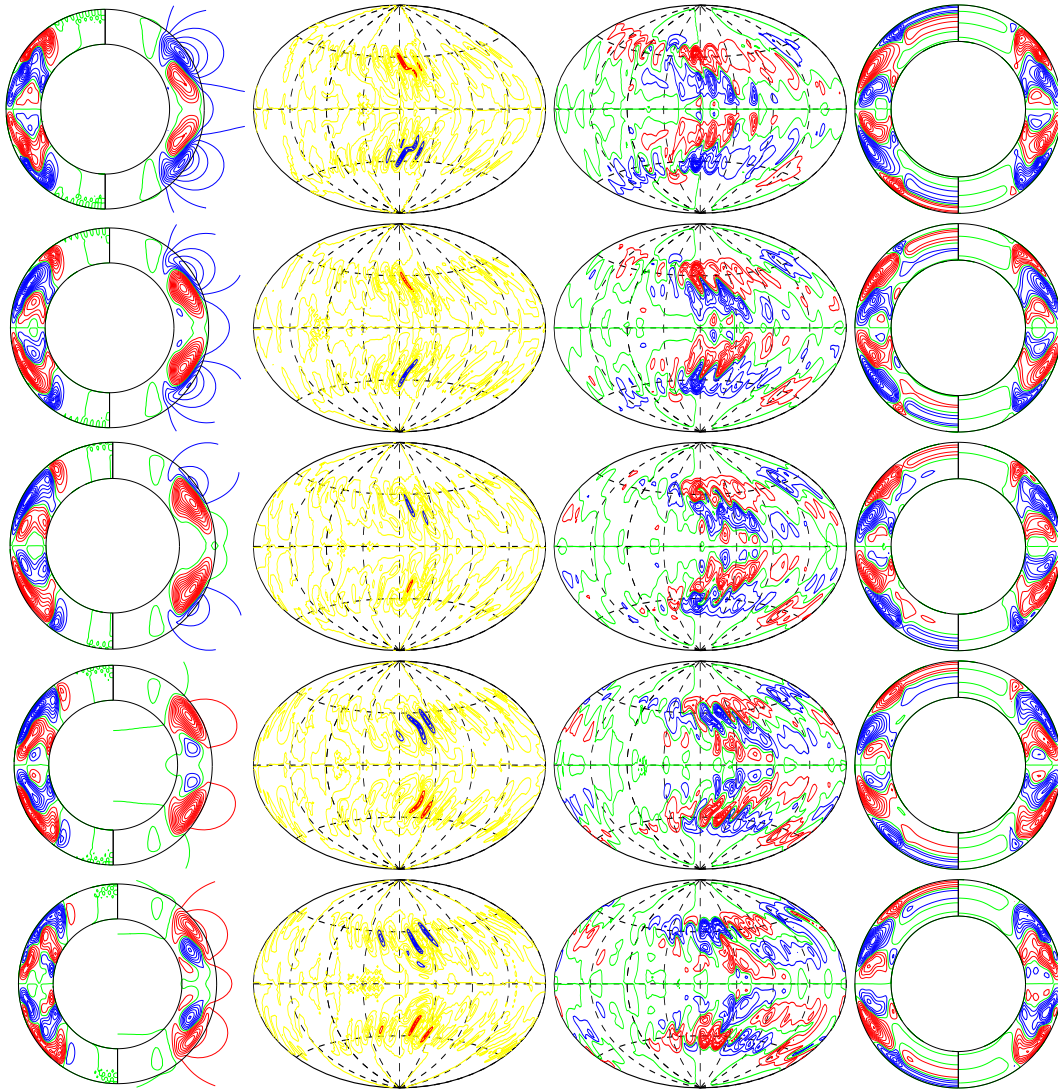


Figure 25: Half a period of oscillation in the case  $\eta = 0.65$ ,  $P = 1.2$ ,  $\tau = 2000$ ,  $R_e = 120000$ ,  $P_m = 4.5$ ,  $\beta = 0$  with stress-free velocity boundary condition at  $r = r_o$  and no-slip at  $r = r_i$ . The first column shows meridional lines of constant  $\bar{B}_\varphi$  to the left and of  $r \sin \theta \partial_\theta \bar{h}$  to the right. Lines of constant  $B_{horiz}$  at  $r = 0.9$ , of  $B_r$  at  $r = 1$  and are shown in the second and third, respectively. The last column shows  $\text{Re}(\partial g^{m=1}/\partial \theta)$  on the left and  $\text{Im}(\partial g^{m=1}/\partial \theta)$  on the right. The time interval between the snapshots is 0.0224.

e065p1.2t2r120000m1p4.5mvbcFD